water

MDPI

Article

Integrated Coagulation–Disinfection Using Aluminium Polychloride and Sodium Hypochlorite for Secondary Wastewater Treatment: Operational Advantages and DBP Mitigation

Naghmeh Fallah [1], Katherine Bell [2], Ted Mao [3,4], Ronald Hofmann [5], Gabriela Ellen Barreto Bossoni [5], Domenico Santoro [6,*] and Giuseppe Mele [1]

[1] Department of Engineering for Innovation, University of Salento, 73100 Lecce, Italy; naghmeh.fallah@unisalento.it (N.F.); giuseppe.mele@unisalento.it (G.M.)
[2] Hazen and Sawyer, 545 Mainstream Drive, Nashville, TN 37228, USA; kbell@hazenandsawyer.com
[3] Research Institute for Environmental Innovation (Suzhou) Tsinghua, Suzhou 215163, China; tedmao@outlook.com
[4] MW Technologies, Inc., London, ON N6K 4V4, Canada
[5] Department of Civil & Mineral Engineering, University of Toronto, Toronto, ON M5S 1A4, Canada; ron.hofmann@utoronto.ca (R.H.); gabi.barretobossoni@utoronto.ca (G.E.B.B.)
[6] CBE Department, University of Western Ontario, London, ON N6A 5B9, Canada
* Correspondence: dsantor@uwo.ca

Abstract

This study examines the potential for improved and more sustainable wastewater treatment by integrating coagulation and disinfection using polyaluminum chloride (PACl) and sodium hypochlorite (NaClO) for secondary effluent. The impacts of this integrated approach on phosphorus removal, microbial inactivation, and disinfection by-product (DBP) formation were evaluated through bench- and pilot-scale experiments under both sequential and simultaneous dosing. The results show that simultaneous dosing of PACl and NaClO achieved high phosphorus removal (>90% at 6–9 mg/L PACl), while microbial inactivation targets were met with moderate chlorine doses (3–6 mg/L). Pilot-scale tests further revealed that PACl enhanced microbial inactivation under high-intensity mixing. Importantly, the integrated process reduced DBP formation substantially, with trihalomethanes (THMs) and haloacetic acids (HAAs) lowered by up to ~50% compared to sequential treatment. By minimizing the need for separate treatment units, shortening hydraulic retention time, and lowering overall chemical consumption, this integrated coagulation–disinfection strategy provides a compact, cost-effective, and sustainable alternative to conventional wastewater treatment.

Keywords: wastewater; integrated process; disinfection; coagulation; DBPs; microbial inactivation; phosphorus removal; bench and pilot scale

Academic Editors: Andrea G. Capodaglio and Jiangyong Hu

Received: 10 August 2025
Revised: 15 September 2025
Accepted: 25 September 2025
Published: 1 October 2025

Citation: Fallah, N.; Bell, K.; Mao, T.; Hofmann, R.; Bossoni, G.E.B.; Santoro, D.; Mele, G. Integrated Coagulation–Disinfection Using Aluminium Polychloride and Sodium Hypochlorite for Secondary Wastewater Treatment: Operational Advantages and DBP Mitigation. *Water* **2025**, *17*, 2867. https://doi.org/10.3390/w17192867

1. Introduction

Sustainable wastewater treatment is essential for protecting public health, conserving water resources, and minimizing environmental impact. Modern treatment systems must not only meet regulatory standards for nutrient removal and pathogen inactivation but also reduce chemical usage, energy demand, and operational footprint. Conventional water treatment typically employs separate steps for coagulation, flocculation, filtration,

and disinfection. While effective, this approach requires considerable space, retention time, and operational resources. From a sustainability perspective, integrating treatment steps could streamline operations, reduce chemical and energy consumption, and enhance overall efficiency.

Coagulation is often conducted using either aluminum or iron-based coagulants such as polyaluminum chloride (PACl), alum, ferric chloride, or ferric sulfate. In particular, polyaluminum chloride (PACl), a pre-hydrolyzed coagulant, is frequently used because of its effectiveness for destabilization of organic matter with a fast rate of particle aggregation during flocculation [1]. With respect to disinfection, chlorine, either as gas or sodium hypochlorite (NaClO), is widely used because of its disinfection efficacy, ability to provide the required residual for distribution and cost-effectiveness. Numerous studies have examined these treatment processes individually, assessing the optimal conditions for their application [2–7]. Noting that it is most common for wastewater treatment plants to perform coagulation and disinfection sequentially [8], this requires each process to have its own space and hydraulic retention time in the treatment facility. From a sustainability perspective, integrating treatment steps offers opportunities to streamline operations, lower environmental footprints, and enhance system efficiency.

Like drinking water treatment, both coagulation and chlorine disinfection are deployed to achieve water quality compliance. Coagulation in wastewater treatment has emerged as a tool for managing total suspended solids as well as for the removal of phosphorus, to protect receiving water bodies from eutrophication [9].

Studies indicate that the hydroxide form of the metal is more effective for phosphorus removal, as it provides reactive surface sites crucial for phosphate adsorption [10]. This suggests that optimizing hydroxide formation could enhance treatment efficiency [11]. While oxidants can influence hydroxide formation for some metals (e.g., Fe-based salts), aluminum in PACl is already present in its highest oxidation state (+3) and cannot be further oxidized by NaClO. Thus, in PACl–NaClO systems, improvements in phosphorus removal are more likely to arise from synergistic interactions with organic matter and microbial inactivation, rather than enhanced hydroxide formation.

Chlorine remains the most widely used disinfectant in wastewater treatment because of its efficacy, cost-effectiveness, and ability to maintain a residual through distribution. Microbial risks, including bacteria, viruses, and protozoa, necessitate reliable disinfection to safeguard public health. The effectiveness of chlorine disinfection depends on both concentration and contact time (CT), and its inactivation kinetics vary depending on the target organisms and water quality conditions. However, chlorine also reacts with effluent organic matter (EfOM) to form disinfection by-products (DBPs) [12], including trihalomethanes (THMs) and haloacetic acids (HAAs). These DBPs are regulated due to health concerns.

Coagulants can interact with EfOM, altering its reactivity. Some researchers have investigated the effect of prior disinfection on coagulation and compared the removal of EfOM by coagulation with and without coagulant, preceding disinfection [13,14]. Several studies show that a reduction of 20–60% in the sum of THM and HAA concentrations can be achieved by using Al-based coagulants in water [8,15,16]. In wastewater, coagulants are typically used for improving settling characteristics and phosphorus removal (REF) [17]. There have also been numerous studies showing that coagulation also removes EfOM in treated wastewater, which can reduce DBP formation in chlorinated effluents (REFS) [17,18]. For example, Ding et al. [19] found that coagulation with $Al_2(SO_4)_3$ reduced haloacetamide formation by 41.8–61.4% by removing DBP precursors from the Huangpu River and a local wastewater plant.

Although there are several studies investigating coagulation and disinfection efficiency over sequential processes, the simultaneous use of these processes has been rarely studied. This study investigates the effectiveness of an integrated coagulation–disinfection process using PACl and NaClO under both bench- and pilot-scale conditions. We evaluate its impact on phosphorus removal, microbial inactivation, and DBP formation compared to the conventional sequential approach. Beyond water quality performance, we explore the sustainability benefits of process integration—including reduced hydraulic retention time, lower chemical demand, and minimized infrastructure requirements—offering a compact and more resource-efficient alternative for next-generation wastewater treatment systems.

2. Materials and Methods

2.1. Secondary Effluent Wastewater Quality

Experiments were conducted on samples collected after secondary clarification at a municipal Wastewater Treatment Plant (WWTP) in Ilderton, Canada. Characteristics of undisinfected secondary effluent are reported in Table 1. Samples were collected using sterile containers to prevent microbial contamination and were transported to a laboratory for testing.

Table 1. Secondary wastewater characteristics.

Parameters	Units	Number of Samples	Min–Max	Average
N-NO_2^-	mg/L	5	0.005–0.008	0.0062
N-NO_3^-	mg/L	5	31.3–38.2	34.8
N-NH_4^+	mg/L	5	0.05–0.07	0.62
Total-N	mg/L	5	25.7–33.9	29.98
COD	mg/L	5	22–45	33.8
Total-PO_4^{3-}	mg/L	5	0.38–2.38	1.54
Reactive-PO_4^{3-}	mg/L	5	0.15–1.26	0.615

Sodium hypochlorite (NaClO), 12.5% *W*/*W* aqueous solution, was purchased from VWR Chemicals BDH, Canada. For experiments, stock solutions of NaClO were prepared by diluting a commercial solution to 0.1% and measuring chlorine concentration using Hach Method 8021 each day prior to testing. Polyaluminium chloride (PACl), Al_2O_3: 10.2 ± 0.3%, was purchased from AQUABOND, Toronto, ON, Canada. For experiments, stock solutions of aqua PACl were prepared by diluting a commercial solution.

2.2. Analytical Methods

The analytical methods employed in this study were selected to evaluate disinfection, focusing on chemical and microbial parameters to assess treatment efficiency and formation of DBPs.

COD was determined using Hach Method 8000 (USEPA reactor digestion method), suitable for 3–150 mg/L. Total nitrogen was determined using Hach Method 10,071 (persulfate digestion method), which can measure 0.5–25 mg/L. Ammonia was measured using Hach Method 10,023 (salicylate method) for a concentration of 0.02–2.5 mg-N/L. Nitrite and nitrate were determined using Hach methods 10,019 and 10,020, respectively. The former, a diazotization method, can measure 0.003–0.5 mg-N/L, while the latter, a chromotropic acid method, is suitable for 0.2–30 mg-N/L. Total phosphorus was analyzed using Hach Method 8190 (USEPA PhosVer® 3 with acid persulfate digestion), suitable for 0.06–3.5 mg/L as PO_4^{3-}. Soluble phosphorus was analyzed using the same method, following filtration with a 0.45-µm nylon filter. Reactive phosphorus was evaluated using Hach method 8148 (USEPA PhosVer®3 method), suitable for 0.06–5.0 mg/L as PO_4^{3-}. During

disinfection experiments, total and free chlorine were immediately measured using Hach Methods 8167 and 8021 for total chlorine and free chlorine, respectively. Both methods are suitable for concentrations of 0–2 mg/L. All colorimetric tests were conducted using a DR3900 laboratory spectrophotometer from Hach (Loveland, CO, USA).

A membrane filtration method was employed for enumeration of total and fecal coliforms with a detection limit of 1 CFU/100 mL. For total coliform, wastewater samples were passed through a 0.45 µm filter and transferred onto mEndo LES agar. Plates were incubated at 35 °C ± 0.5 °C for 18–24 h. Fecal coliforms were measured using Standard Methods for the Enumeration of Water and Wastewater (9222 D), which includes sample filtration through a 0.45 µm filter, placed onto mFC agar. Fecal coliforms were incubated at 44.5 ± 0.2 °C for 24 ± 2 h.

The DBPs evaluated for this study included trihalomethanes (THMs), haloacetic acids (HAAs), haloacetonitriles (HANs), haloketones (HKs), and haloaldehydes (HALs), which were extracted and analyzed using liquid–liquid extraction and gas chromatography–electron capture detection, following EPA Methods 551.1 and 552.3. Adsorbable organic halides (AOX) were determined using an AOX analyzer (Model: Xplorer, TE Instruments, Amsterdam, The Netherlands). Table S6 shows the list of monitored DBPs in our case study.

2.3. Experimental Procedures

2.3.1. Bench Scale Testing

Several series of experiments were designed to investigate the impact of simultaneous application of PACl as a coagulant and NaClO as a disinfectant under low-mixing conditions, on phosphorus removal, microbial inactivation and DBP formation. Experiments were conducted in beakers, utilizing 1000 mL of undisinfected secondary wastewater effluent. A magnetic stir bar was used to mix samples at an ambient temperature of 25 ± 2 °C. The PACl and NaClO solutions were prepared on the day of the assay and were stored in a tightly sealed glass bottle prior to use. The calculated G-value for these experiments was around 762 s^{-1} at atmospheric pressure.

Screening experiments were conducted for integrated treatment at low-mixing conditions used varying quantities of NaClO (3, 4.5, and 6 mg/L) with various concentrations of PACl. Following 21 s of mixing with a stirring speed of around 1100 rpm, samples were collected for analyses of soluble phosphorus. Experiments were repeated for water collected on five different days. For sequential treatment screening experiments, and for screening disinfection experiments, varying doses of chlorine (3, 4.5, and 6 mg/L) and various amounts of PACl were added to the wastewater sample simultaneously. Following three mixing times (14, 21, and 29 s), samples were then collected for analysis. The analysis of each sample involved measuring the levels of total coliform and fecal coliform, as well as DBP concentrations. A summary of experiments is presented in Table 2.

Table 2. Summary of the experimental design for the batch experiment.

Series. *n*	NaClO Dose (mg/L)	PACl Dose (mg/L)	Process Time	Outcome
1	3	0, 3, 6	21 s mixing	Soluble phosphorus
2	4.5	0, 4.5, 9	21 s mixing	Soluble phosphorus
3	6	0, 6, 12	21 s mixing	Soluble phosphorus
4	3	0, 3, 6	14, 21, 29 s mixing	Total coliform, Fecal coliform, DBPs
5	4.5	0, 4.5, 9	14, 21, 29 s mixing	Total coliform, Fecal coliform, DBPs
6	6	0, 6, 12	14, 21, 29 s mixing	Total coliform, Fecal coliform, DBPs

The wastewater used in each test was collected fresh on the day of the experiment and was not stored prior to testing. Samples were analyzed immediately after the designated mixing time: general water quality parameters were measured directly, while aliquots were sent for DBP and microbial analysis. To ensure reproducibility, the experiments were repeated on five separate days using independently collected wastewater samples. In all tests, chlorination was terminated by adding a solution of sodium metabisulfite. To determine the optimal amount of sodium metabisulfite needed to stop the chlorination process, several experiments were conducted. Using the maximum NaClO dose applied in our study (6 ppm) as the initial NaClO concentration, various doses of sodium metabisulfite (6, 9, 12, 15 ppm) were added to the solution. The results indicated that chlorination was effectively terminated with a sodium metabisulfite solution at a 2:1 ratio relative to chlorine. In the experiments, sodium metabisulfite was added according to this optimized ratio and confirmed by chlorine residual testing.

2.3.2. Pilot Scale Testing

Integrated disinfection/coagulation experiments were conducted in a specially designed system, which included two pumps and two $MITO_3X$ multifunctional reactors to provide high-mixing conditions ($\bar{G} \approx 10{,}000\ s^{-1}$ at 1.5 atm). The experimental setup is depicted in Figure 1.

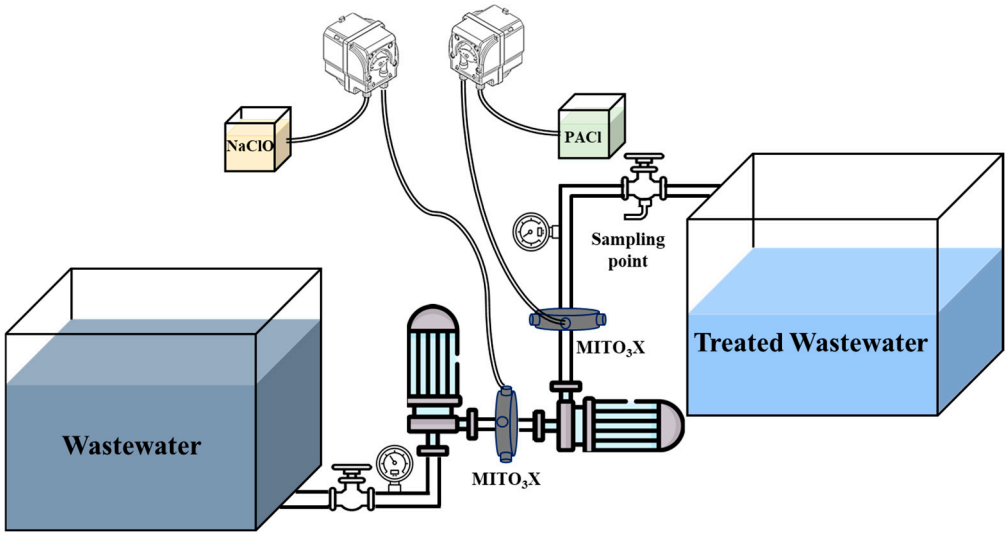

Figure 1. A visual representation of pilot experimental setup.

The feed tank was filled with undisinfected secondary wastewater effluent to supply the treatment process. Operation of the system was controlled by adjusting valves to modify the flow rate of the pilot feed. The sample was directed through a series of two centrifugal pumps and two compact $MITO_3X$ multifunctional reactors. This unique configuration facilitates continuous introduction of the oxidant (NaClO) and coagulant into the system, which also provides high mixing, thus improving interaction between chemicals and feed water. Pressure gauges were installed at various points in the system, with sample ports being strategically placed to allow collection of treated samples. Varying doses of PACl and NaClO were continuously pumped into the $MITO_3X$ multifunctional reactors. Flow rates were controlled using a peristaltic pump for precise control over the process.

Experiments were conducted by adjusting the wastewater flow rates (3.7, 8 and 12 L/h) and varying the speed of the peristaltic pump for injecting PACl and NaClO solutions. Specific pump speeds, when used with each constant wastewater flow rate, correspond to a series of chemical doses. Immediately after mixing, samples were collected for analysis.

Similarly to the bench-scale tests, fresh wastewater was collected and used immediately on the day of the experiment. Samples were analyzed directly after mixing, with portions sent for DBP and microbial analyses. Each operating condition was tested in duplicate to confirm consistency of results. The analyses of each sample included total coliform, fecal coliform, and DBPs. Chlorination was terminated by introducing a solution of sodium metabisulfite.

Detailed specifications of the batch- and pilot-scale experimental setups, including mean velocity gradient (G) calculations, G·t values, hydraulic retention times, and sample collection procedures, are provided in Fallah et al. (2025) [20].

3. Results

Preliminary experiments were conducted to assess whether combining disinfection and coagulation processes would impact the efficiency of each process independently under low-mixing conditions. To provide additional clarification on the batch experimental design, a summary of each experimental series is presented in Table S1. Experimental data comparing sequential and simultaneous disinfection/coagulation approaches (Figures S1 and S2) indicate that the removal efficiency for soluble phosphorus and total coliform inactivation remains largely consistent across different treatment schemes under low-mixing conditions setups. Integrating these processes (using PACl for coagulation and NaClO for disinfection) in a single reactor could reduce both facility footprint and hydraulic demands by streamlining these unit processes. Future research will explore this combined approach further, with the goal of developing more advanced treatment technologies that achieve regulatory compliance with reduced spatial and hydraulic requirements.

3.1. Phosphorus Removal

To assess integrated disinfection and coagulation at the bench scale, experiments involved the manipulation of three critical parameters: the dose of PACl and NaClO and mixing time at low-mixing energy. The primary focus was to examine the relationships among these parameters, and their impact on phosphorus removal, microbial inactivation, and DBP formation. To analyze the complex interplay of these factors, a robust multivariate statistical analysis was conducted using the Design-Expert® software package. To explore the effects of integrated PACl and NaClO treatment at bench scale on phosphorus removal efficiency, varying doses of PACl and NaClO were simultaneously introduced into undisinfected secondary wastewater effluent. After 21 s low-mixing, soluble phosphorus was measured; the results are presented in Table S2. A multivariate statistical analysis was conducted assessing PACl and NaClO doses as independent variables, with soluble phosphorus as the response variable. An ANOVA test yielded the coefficient of determination (R^2), adjusted R^2, predicted R^2, and standard deviation, which are summarized in Table 3. ANOVA summary tables and actual vs. predicted plots for all models are provided in the Supporting Information (Table S7 and Figure S6). The equation predicting response, based on NaClO and PACl doses, is provided below:

$$C_{Soluble\ P} = 0.242209 + 0.005688\ C_{NaClO} - 0.03607\ C_{PACl} + 0.002086\ C_{PACl}^2 \quad (1)$$

where $C_{Soluble\ P}$ represents the final concentration (after treatment) of soluble phosphorus and C_{NaClO} and C_{PACl} are initial concentrations of NaClO and PACl, respectively, all in mg/L.

Table 3. Statistical values of phosphorus removal model.

Parameter	Value
Model	Quadratic
R^2	0.67
Adjusted R^2	0.65
Predicted R^2	0.60
Std. Dev.	0.046

Additional model validation was performed using profile plots of soluble phosphorus removal (Figure 2). The results showed that phosphorus removal in the integrated PACl/NaClO process was controlled primarily by the coagulation step. PACl hydrolyzes to form positively charged aluminum hydroxide species that bind and precipitate phosphate (negatively charged) via charge neutralization [21]. In our experiments, increasing the PACl dose initially enhanced soluble-P removal (approaching 90%+), but beyond an optimum (around 9 mg/L) the removal efficiency leveled off or even declined slightly. This diminishing return at high coagulant dose is a well-known phenomenon: once colloids and phosphate ions are neutralized, excess aluminum can lead to charge reversal or the re-stabilization of particles [21]. In other words, overdosing PACl may oversaturate active sites or invert particle surface charge, thus reducing floc aggregation and settling. Thus, our observations of reduced P removal at very high PACl doses are consistent with general colloid chemistry and prior studies of chemical phosphorus precipitation [22–24].

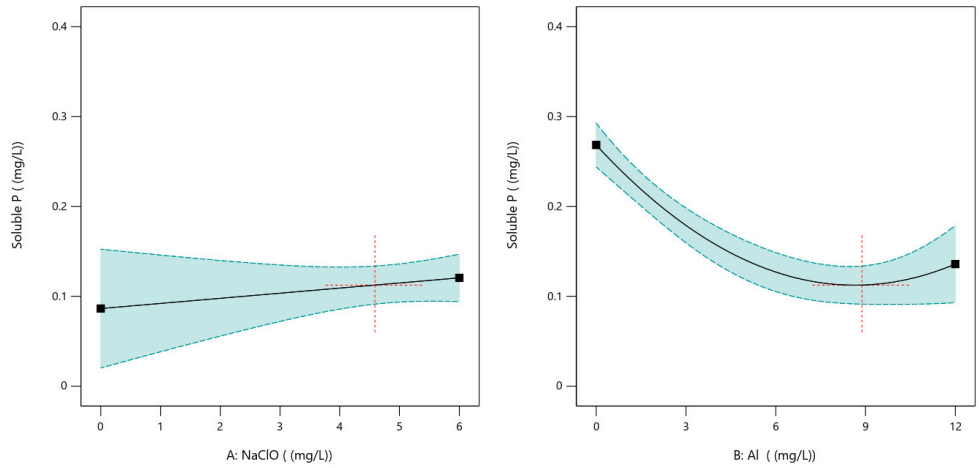

Figure 2. Profile plots of phosphorus removal. Panel (**A**): NaClO dose, Panel (**B**): PACl dose.

Adding NaClO had only a minor negative impact on P removal. At a fixed PACl dose (6 mg/L), increasing NaClO from 0 to 6 mg/L caused a very small rise in soluble P. One possible explanation is that the chlorine oxidant altered the particle surface chemistry. It is known that pre-oxidants like chlorine can strip organic coatings and change zeta potential, which can either enhance or inhibit coagulation. In fact, pre oxidation is often intended to "vary the zeta potential" by destroying organic coatings on particle surfaces, thereby promoting aggregation [21]. In our wastewater matrix, however, any potential beneficial pre oxidation effect of NaClO on coagulation was outweighed by slight destabilization: the data suggest that NaClO induced subtle charge, and possibly minor pH variations, that marginally reduced floc formation. Since pH was not systematically measured across all experiments, this explanation should be considered tentative and will be investigated further in future work. This aligns with prior reports that chlorine pre-oxidation may improve algae coagulation under some conditions, but in our case the effect was small.

Importantly, the NaClO doses used were low relative to PACl, and the overall P removal remained high, indicating that disinfection dosing did not substantially interfere with coagulation under the studied conditions.

We did not directly measure zeta potential in this study, but the literature on aluminum coagulation suggests that optimal phosphorus removal corresponds to near-neutral zeta potential of colloids. Beyond this point, the system can invert charge. Our results imply that PACl dosing should be carefully optimized: using design-of-experiments, the models indicate an optimal PACl range (6–9 mg/L) for maximum P uptake, consistent with typical stoichiometric requirements. Lowering pH into the 5–7 range (the ideal range for Al phosphate precipitation) could further improve removal if the plant effluent pH permits. In summary, efficient P removal in the integrated process relies on achieving the right PACl dose—enough to neutralize and precipitate phosphate, but not so much as to reverse particle charge—while recognizing that NaClO co dosing has only a minor, secondary effect on this mechanism.

3.2. Microbial Inactivation

To assess the efficiency of microbial inactivation resulting from the integration of PACl and NaClO treatment in the bench-scale tests under low mixing energy, varying concentrations of NaClO (3, 4.5, and 6 mg/L) and PACl were simultaneously added to samples. Three mixing intervals (14, 21, and 29 s) were tested, and total and fecal coliform bacteria were measured; the results are presented in Table S3. In the bench-scale tests under low mixing, microbial inactivation was dictated almost entirely by NaClO dose, with PACl exerting no observable effect. Both total and fecal coliform log-reductions scaled with chlorine concentration, as expected in a conventional chlorination scenario. This matches the finding of Hu et al. [25] that dual Al-Cl reagents (E-PACl) rely on the active chlorine content to kill pathogens. Thus, at small scale with minimal turbulence, PACl acted only as a passive particle remover and did not contribute to disinfection. By contrast, in pilot-scale tests with high mixing energy, a clear synergy between PACl and NaClO emerged. Increasing PACl dose (at fixed NaClO) improved coliform inactivation (Table S4).

A multivariate statistical analysis was used to elucidate which parameters impacted microbial inactivation. Factors considered at the bench scale included PACl and NaClO doses, as well as mixing time, and factors considered at the pilot scale included PACl and NaClO doses, and wastewater flowrate. Total and fecal coliform inactivation was set as the treatment response. Results from an ANOVA, including the coefficient of determination (R2), adjusted R2, predicted R2, and standard deviation, are presented in Table 4. ANOVA summary tables and actual vs. predicted plots for all models are provided in the Supporting Information (Tables S8–S11 and Figures S7–S10). Final equations for total and fecal coliform inactivation at the bench scale and pilot scale in terms of actual factors are the predicted the response for given level of each factor, as shown in Table 5.

Table 4. Statistical values of total and fecal coliform inactivation model.

	Bench Scale		**Pilot Scale**	
Parameter	**Fecal Coliform**	**Total Coliform**	**Fecal Coliform**	**Total Coliform**
Model	Linear	Linear	Linear	Linear
R^2	0.59	0.82	0.6	0.56
Adjusted R^2	0.57	0.80	0.58	0.54
Predicted R^2	0.52	0.76	0.5	0.47
Std. Dev.	0.35	0.26	0.12	0.23

Table 5. Final equations for total and fecal coliform inactivation in each treatment system.

Bench Scale	
$log(\frac{N_0}{N})_{Fecal\ coliform}$	$= 1.28574 + 0.327778\ C_{NaClO}$
$log(\frac{N_0}{N})_{Total\ coliform}$	$= 0.084342 + 0.327909\ C_{NaClO} + 0.050289\ t$
Pilot Scale	
$log(\frac{N_0}{N})_{Fecal\ coliform}$	$= 3.55757 + 0.036569\ C_{PACl}$
$log(\frac{N_0}{N})_{Total\ coliform}$	$= 3.34298 + 0.063692\ C_{PACl}$

In these equations, C_{NaClO} and C_{PACl} are initial concentrations of NaClO and PACl, respectively, measured in mg/L. t stands for mixing time in the unit of minutes. $log(\frac{N_0}{N})_{Fecal\ coliform}$ and $log(\frac{N_0}{N})_{Total\ coliform}$ represent the normalized logarithmic reduction in fecal coliform and total coliform population. N_0 and N represent the initial concentration of coliform bacteria before and after treatment, respectively.

Additional validation was conducted using graphical techniques; Figure 3 illustrates fecal coliform inactivation, while Figure 4 presents total coliform inactivation at the bench scale. Leveraging both the model and graphical analyses, fecal coliform inactivation depends only on the NaClO concentration; however, total coliform inactivation also depends on mixing time.

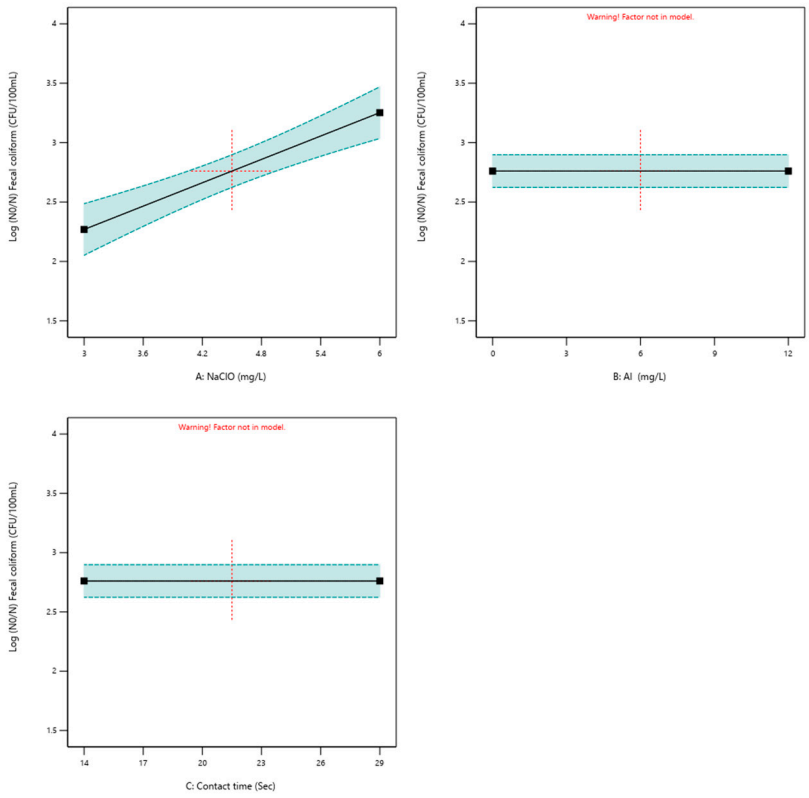

Figure 3. Profile plots of fecal coliform inactivation. Panel (**A**): NaClO dose, Panel (**B**): PACl dose, Panel (**C**): contact time.

In the figures generated using Design-Expert software (version: 23.1), the black dots represent the range of actual measured data points, the blue shaded area shows the confidence interval of the model prediction, and the red dashed line indicates the center point of the factor in the design. The red text ("Warning! Factor not in model") appears when the factor plotted was not included in the statistical model for that response.

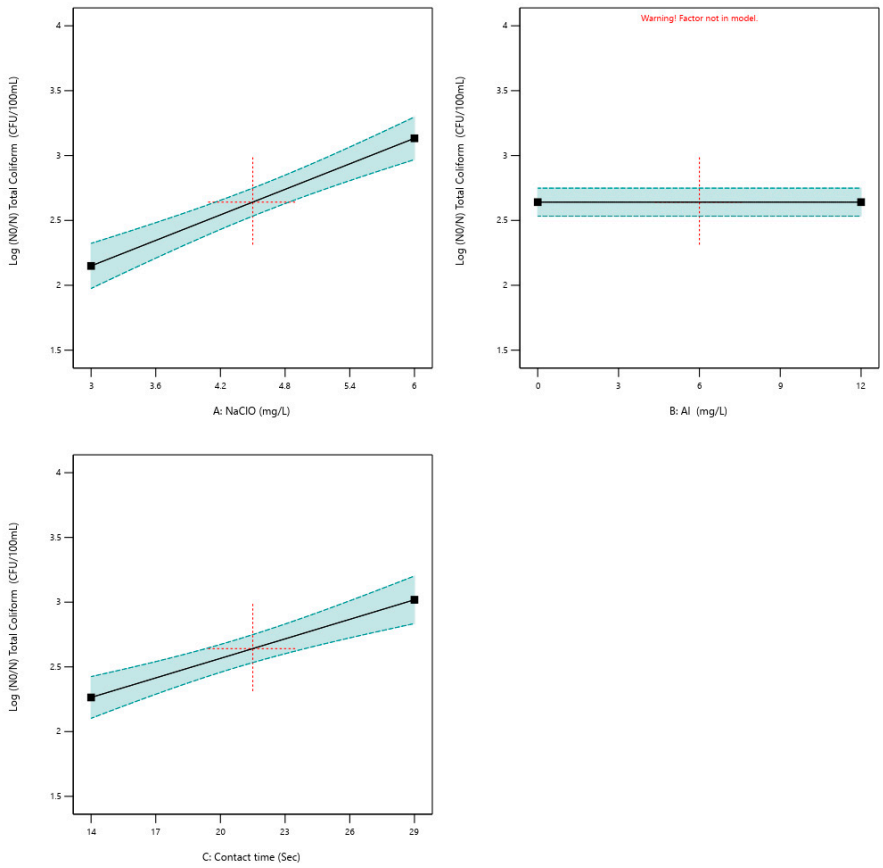

Figure 4. Profile plots of total coliform inactivation. Panel (**A**): NaClO dose, Panel (**B**): PACl dose, Panel (**C**): contact time.

Figures 5 and 6 illustrate fecal and total coliform inactivation as a function of NaClO and PACl doses at the pilot scale. Results demonstrate that inactivation of coliform bacteria is highly influenced by the PACl, with improved inactivation as PACl doses are increased. For example, at 3 mg/L NaClO, the total coliform reduction improved from ~72% (PACl 0) to ~81% (PACl 6 mg/L), and at 6 mg/L NaClO, the fecal coliform kill increased from 77% to 91% as PACl rose from 0 to 12 mg/L. This synergistic effect likely arises because PACl flocs can enmesh or co-precipitate bacteria, exposing them to disinfectants for longer or shielding them from pipe wall losses. High shear mixing in the $MITO_3X$ reactor further enhanced contact between oxidant, flocs, and microorganisms. Similar dual-function reagents have demonstrated this phenomenon: Hu et al. [25] reported that an electrochemically prepared PACl with built-in active chlorine was able to achieve simultaneous coagulation and near-complete coliform inactivation. In practical terms, the integrated high-mix system boosted disinfection efficacy without additional chlorine. It appears that at high turbulence the coagulant provides sites for reactive chlorine species to attack clustered organisms, thereby amplifying kill rates.

Overall, these findings indicate that simultaneous dosing can preserve or even enhance disinfection performance. At the bench scale, we verified that conventional chlorine kinetics apply (PACl presence did not hamper NaClO kill), while at the pilot scale we observed a clear benefit of coagulant flocs on disinfection. This demonstrates that an integrated PACl/NaClO process can maintain regulatory log-removal requirements for pathogens (through appropriate NaClO dosing) and may allow for lower chlorine doses in practice due to synergistic effects.

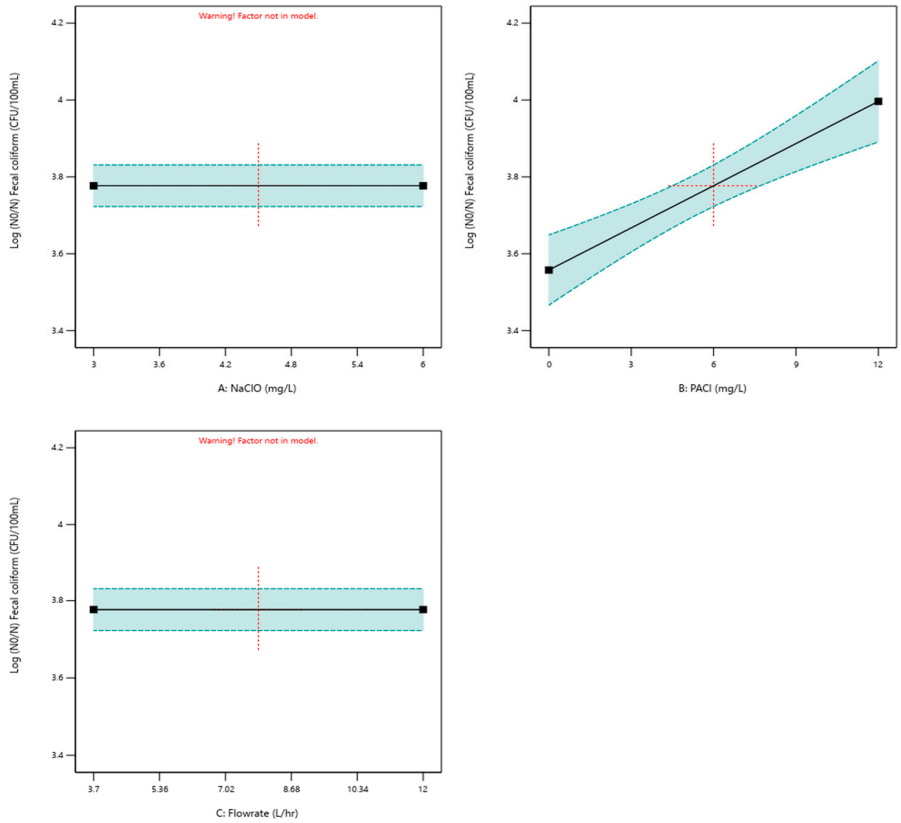

Figure 5. Profile plots of fecal coliform inactivation. Panel (**A**): NaClO dose, Panel (**B**): PACl dose, Panel (**C**): flowrate.

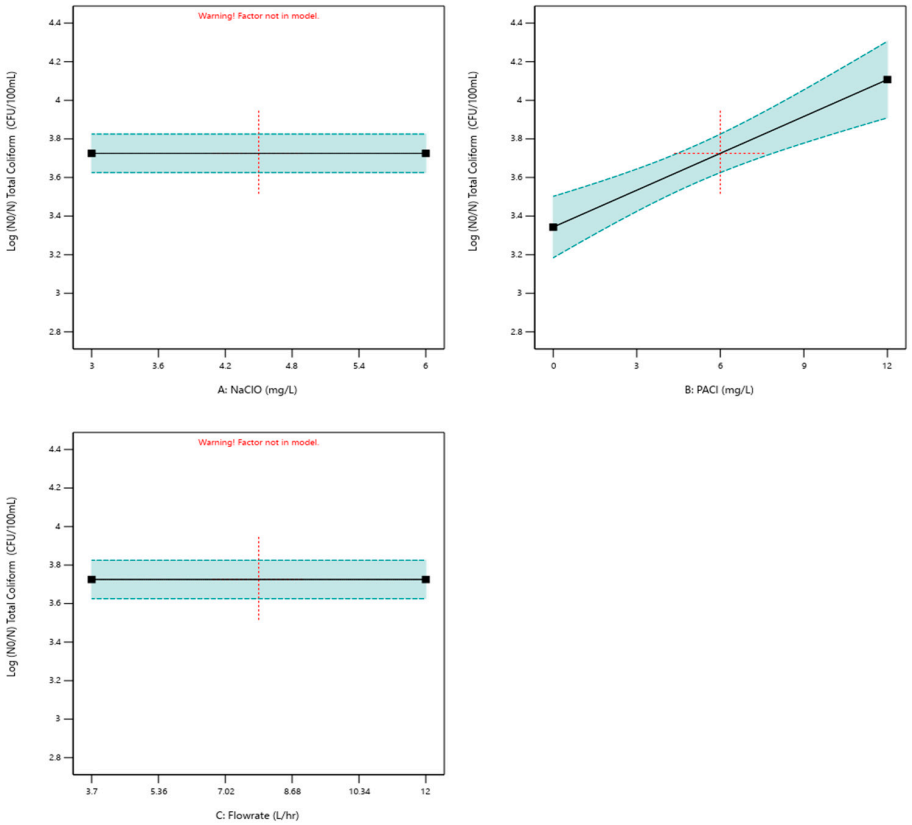

Figure 6. Profile plots of total coliform inactivation. Panel (**A**): NaClO dose, Panel (**B**): PACl dose, Panel (**C**): flowrate.

3.3. DBP Formation

To evaluate DBP formation at the bench scale, with low-mixing conditions, varying concentrations of NaClO and PACl were dosed simultaneously. After mixing at three intervals (14, 21, and 29 s), samples were collected and analyzed, with the results presented in Table S3. Of the six DBP categories, HANs and AOX did not exhibit dependency on any variables. The other four DBPs, however, showed response relationships that are discussed here. On the other hand, to evaluate DBP formation in the pilot system over different flowrates, varying concentrations of NaClO and different amounts of PACl were injected into a wastewater flow simultaneously; the results are shown in Table S5.

A multivariate statistical analysis was applied to elucidate which parameters impact DBP formation. At the bench scale, PACl and NaClO doses, as well as mixing time, were evaluated as independent parameters, while the THMs, HAAs, HALs, and HKs were set as response parameters. At the pilot scale, PACl and NaClO doses, and wastewater flowrate were independent factors, while THMs, HAAs, AOX, HANs, HALs, and HKs were assessed as treatment response parameters. ANOVA summary tables and actual vs. predicted plots for all models are provided in the Supporting Information (Tables S12–S19 and Figures S11–S18). The model results and final equations are presented in Tables 6 and 7, respectively, for the monitored DBPs under each treatment system.

Table 6. Statistical values of monitored DBP model.

	Bench Scale				**Pilot Scale**					
Parameter	**THMs**	**HAAs**	**HALs**	**HKs**	**THMs**	**HAAs**	**AOX**	**HANs**	**HALs**	**HKs**
Model	2FI	2FI	2FI	Linear	Quadratic	Quadratic	Quadratic	Quadratic	Quadratic	Quadratic
R^2	0.35	0.61	0.6	0.77	0.98	0.87	0.75	0.96	0.9	0.95
Adjusted R^2	0.29	0.54	0.5	0.74	0.97	0.86	0.66	0.95	0.89	0.94
Predicted R^2	0.14	0.46	0.43	0.69	0.96	0.83	0.46	0.94	0.84	0.91
Std. Dev.	4.01	1.63	0.14	0.1	0.41	1.85	21.11	0.24	0.26	0.18

Table 7. Final equations for each DBP under each treatment system.

Bench Scale
$C_{THMs} = 16.94987 - 0.325248\ t + 0.008493\ C_{PACl}\ t$
$C_{HAAs} = 3.40496 + 3.89001\ C_{NaClO} + 0.468633\ t - 0.115703\ C_{NaClO}\ t$
$C_{HALs} = 5.58503 + 0.394025\ C_{NaClO} - 0.018749\ C_{PACl} + 0.065505\ t - 0.015515\ C_{NaClO}\ t$
$C_{HKs} = 6.66347 + 0.130081\ C_{NaClO} - 0.026566\ C_{PACl} - 0.0105\ t$
Pilot Scale
$C_{THMs} = 27.60678 - 1.32458\ C_{NaClO} - 3.41956\ Q + 0.176111 C_{NaClO}^2 + 0.246996\ Q^2$
$C_{HAAs} = 42.50040 - 0.200604\ C_{PACl} - 4.41742\ Q + 0.206727\ Q^2$
$C_{AOX} = 382.85542 - 9.80655\ C_{NaClO} - 6.38124\ C_{PACl} - 57.07231\ Q + 2.31072\ C_{NaClO} Q + 0.646007\ C_{PACl} Q + 2.94541 Q^2$
$C_{HANs} = 8.41044 - 0.61908\ C_{NaClO} - 1.05224\ Q + 0.08552\ C_{NaClO}^2 + 0.049329\ Q^2$
$C_{HALs} = 11.91727 - 0.053787\ C_{NaClO} - 0.938728\ Q + 0.938728\ Q + 0.028374\ C_{NaClO} Q + 0.04038\ Q^2$
$C_{HKs} = 10.04305 + 0.206629\ C_{NaClO} - 0.017099\ C_{PACl} - 0.6598\ Q + 0.029934\ Q^2$

In these equations,

- C_{NaClO} and C_{PACl} are initial concentrations of NaClO and PACl (mg/L), respectively.
- t is mixing time (minutes).
- Q represents wastewater flowrate (L/hr).

- C_{THMs}, C_{HAAs}, C_{AOX}, C_{HANs}, C_{HALs}, and C_{HKs} are the post-treatment concentrations of THMs, HAAs, AOX, HANs, HALs, and HKs, respectively (μg/L).

Additional validation was performed using graphical techniques, as shown in Figures 7 and 8 and Figures S3 and S4, which illustrate profile plots at the bench scale for THMs, HAAs, HALs, and HKs, respectively. The integrated process substantially reduced the formation of regulated DBPs (THMs, HAAs) compared to chlorination alone. In the bench tests, THMs were influenced by both PACl dose and contact time: higher PACl consistently suppressed THM formation, and the simultaneous addition of PACl with NaClO produced a synergistic reduction. For instance, at 3 mg/L NaClO and 29 s mixing, raising PACl from 0 to 3 mg/L cut THMs by 56%, and similarly at 4.5 mg/L NaClO, a 47% drop was seen (Figure 7). Over longer contact, the effect intensified (19 to 6.1 μg/L THM from 14 to 29 s under maximum dosing). These results align with the well-documented role of aluminum coagulation in removing DBP precursors. The literature shows that Al-based coagulants preferentially remove hydrophobic, higher-molecular-weight fractions of effluent organic matter (EfOM)—specifically the humic-like and neutral organics that are THM/HAA precursors [26,27]. Song et al. [26] reported that coagulation removed mainly the hydrophobic base (HOB) and neutral (HON) fractions of EfOM, leading to much lower THM and HAA formation potentials. In our tests, the drop in THMs with PACl addition is consistent with this mechanism: by co-precipitating humic substances, the integrated process limits the chlorination substrates that generate THMs.

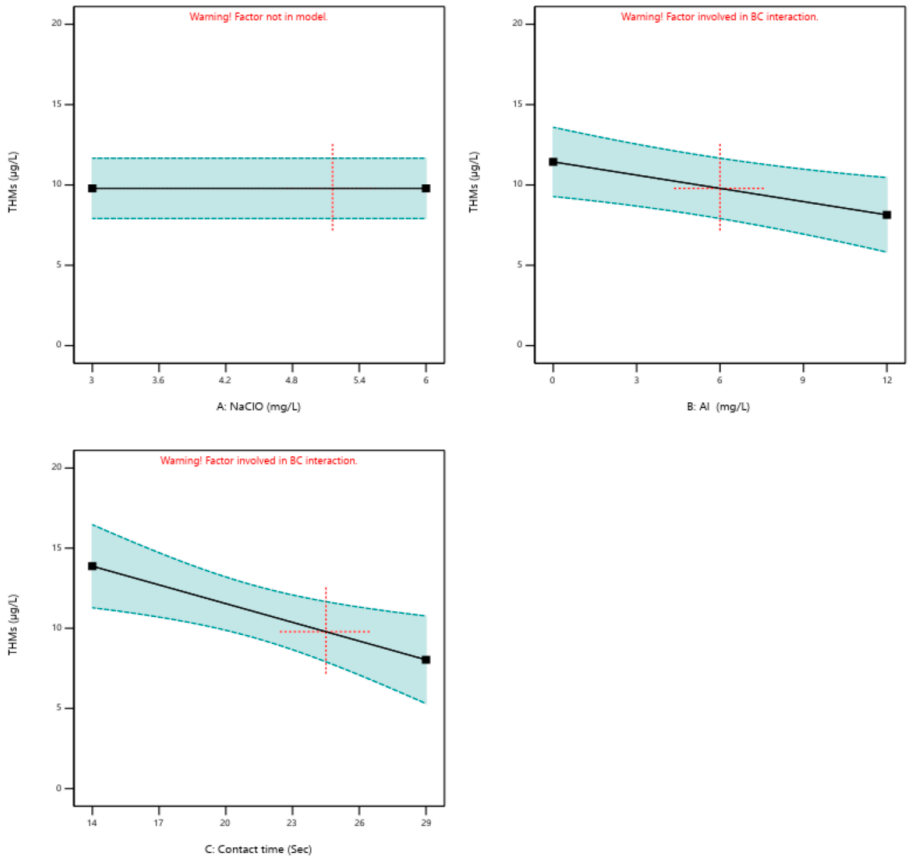

Figure 7. Profile plots of THM formation. Panel (**A**): NaClO dose, Panel (**B**): PACl dose, Panel (**C**): contact time.

Likewise, HAAs were primarily driven by NaClO dose (more chlorine gave more HAAs), but co-addition of PACl still curtailed HAA yields. This likely reflects the removal of hydrophobic organic carbon by coagulation, which shifts the NOM toward more hydrophilic components and lowers HAA precursors [27,28]. The bench-scale results showed

that HAL and HK formation had similar trends with respect to the integrated coagulation/disinfection process (Figures S3 and S4). HAL and HK formation is influenced by all three parameters examined: chemical contact time, and the doses of PACl and NaClO. There is a relationship between coagulation and disinfection in HAL and HK formation. The results show that increasing doses of PACl reduces HAL and HK formation. Interestingly, when NaClO is used simultaneously with PACl, a synergistic effect emerges, and this approach reduces HAL and HK formation. Extending the time under low-mixing conditions amplifies the benefits of the integrated process, producing lower HAL and HK concentrations [17,19,29–31].

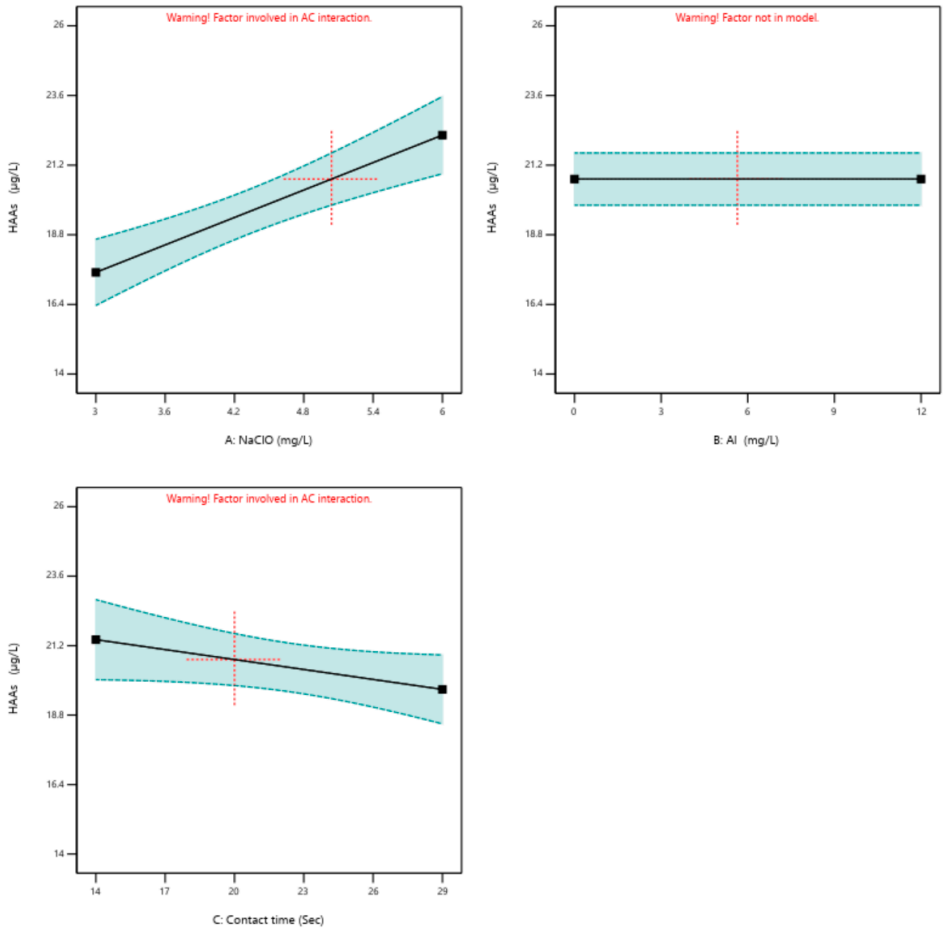

Figure 8. Profile plots for HAA formation. Panel (**A**): NaClO dose, Panel (**B**): PACl dose, Panel (**C**): contact time.

To further examine the role of individual variables, we applied one-factor-at-a-time graphical evaluation (Figures 9 and 10 and Figure S5). These plots illustrate the effects of NaClO and PACl doses, as well as wastewater flowrate, on THM, HAA, AOX, HAN, HAL, and HK formation in pilot-scale experiments. Increasing the NaClO dose raised THM, AOX, HAN, HAL, and HK formation, whereas PACl addition reduced the overall DBP formation potential under high-mixing conditions. Notably, PACl had no significant effect on THMs, HALs, and HANs in the pilot tests, suggesting that the remaining precursors for these DBPs were either abundant or less affected by coagulation. However, HAAs, AOX, and HKs did decrease with higher PACl. For example, at 6 mg/L NaClO and 21 s, adding 6 mg/L PACl cut AOX by ~4% (and 12 mg/L PACl by ~5%). These modest reductions indicate diminishing returns at higher PACl, but confirm the trend that coagulation removes some residual organic load (as measured by AOX and HAA precursors).

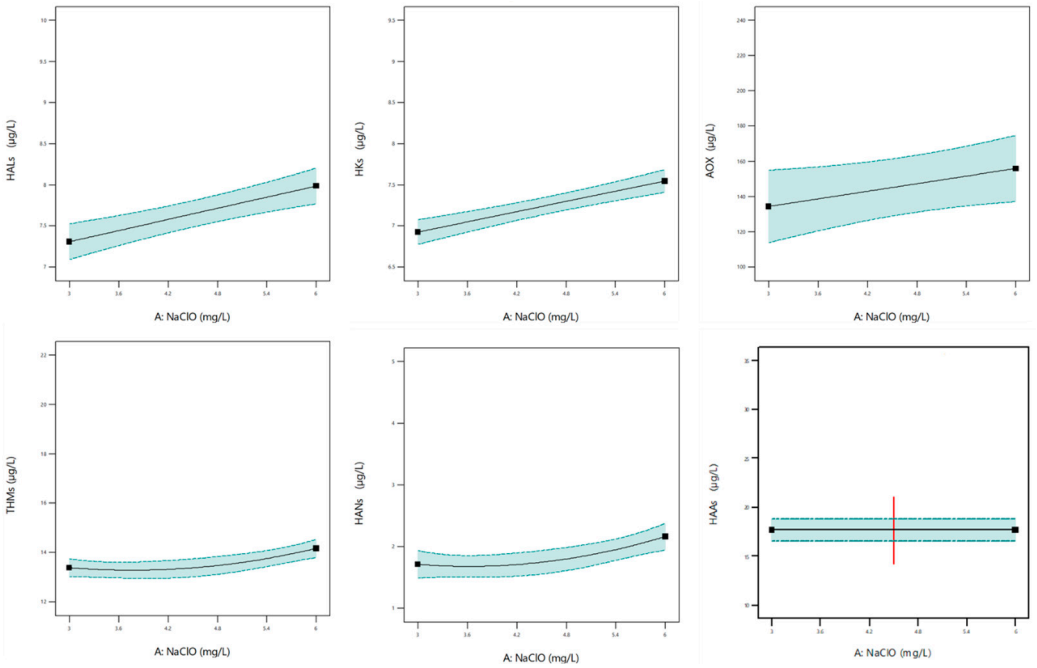

Figure 9. Profile plots of THM, HAA, AOX, HAN, HAL, and HK formation.

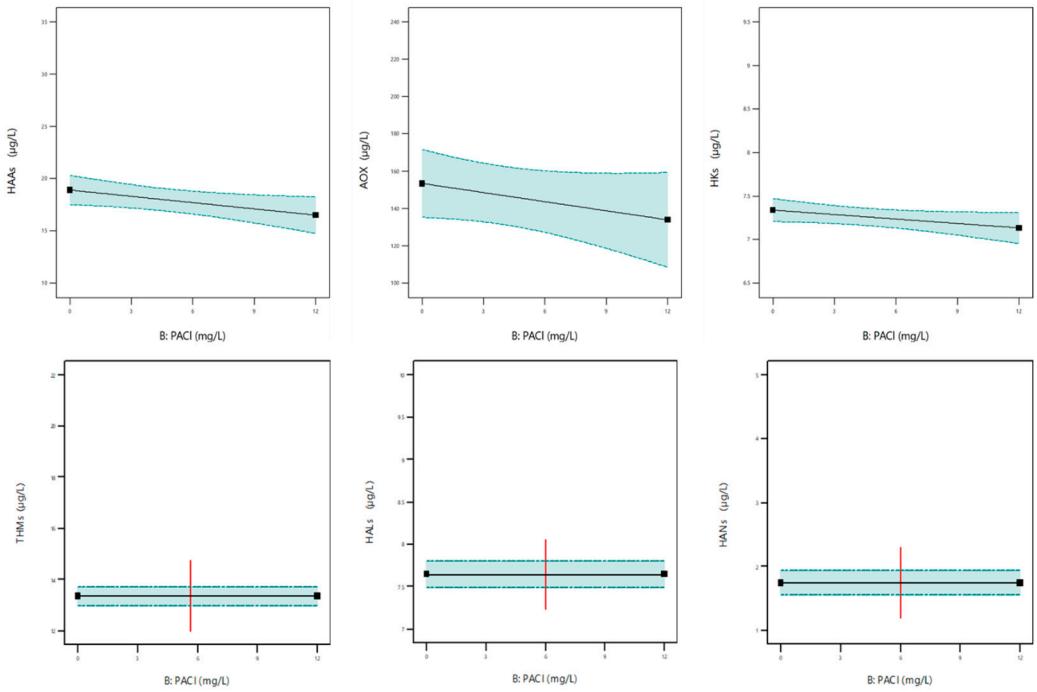

Figure 10. Profile plots of THMs, HAAs, AOX, HANs, HALs, and HKs formation.

Because we did not characterize organic fractions in the water directly, we relied on related studies to interpret these DBP trends. Prior research shows that coagulation tends to convert hydrophobic organics into humic/fulvic forms (as seen by changes in EEM spectroscopy) and greatly reduces high-MW fractions [26,28]. For example, Wang et al. [28] found >90% removal of the hydrophobic neutral fraction (HON) after PACl treatment and noted a shift in the composition of ensuing HAAs. By analogy, our integrated PACl/NaClO likely shifted the EfOM composition toward lower-reactivity species. The graphical profile plots (Figures 9 and 10) support this: the combined process resulted in consistently lower THM and HAA levels than chlorination alone for comparable chlorine doses.

Importantly, while we observed reductions in conventional DBPs, we did not measure DBP toxicity. Regulatory frameworks (e.g., the U.S. EPA Stage 2 DBP Rule) focus on THM and HAA limits, and our integrated approach clearly helps meet such rules by lowering precursor load [27]. However, emerging evidence suggests many DBPs—especially nitrogenous DBPs—may pose higher health risks. Kalita et al. [32] cataloged dozens of DBPs with significant toxicity potential and urged more comprehensive monitoring. Likewise, ecotoxicological reviews have shown that disinfected effluents rich in DBPs can harm aquatic life even when coliform levels are low [33]. Although our integrated approach reduces regulated DBPs, future work should directly assess toxicity endpoints. Approaches such as in vivo bioassays or risk-based guidelines would verify whether these reductions translate into lower ecological and health hazards in treated waters.

Moreover, the observed reductions in DBPs, although modest, are meaningful from both a public health and environmental perspective. Lower DBP concentrations can reduce the potential risks associated with long-term exposure, including carcinogenic and mutagenic effects. From an environmental standpoint, decreased DBP formation can lessen the impacts on receiving water bodies and aquatic organisms. These findings underscore the potential benefits of the integrated PACl/NaClO treatment strategy in improving compliance with regulatory limits and enhancing overall water quality [34–36].

4. Practical Implications

The integrated coagulation–chlorination approach offers several advantages for full-scale wastewater treatment. By dosing PACl and NaClO concurrently in a single reactor, the process merges coagulation and disinfection into one step. This reduces plant footprint, infrastructure demands, and capital costs, while shortening the hydraulic retention time. For example, the MITO$_3$X high-mix reactor functioned as a combined flocculation/disinfection tank, eliminating the need for separate clarifiers or chlorine contact tanks.

Operationally, the process supports efficient and sustainable treatment. Our models (Table 5) show that moderate PACl doses (6–9 mg/L) achieve high phosphorus uptake and DBP precursor removal, while synergy with NaClO enables effective microbial inactivation at lower chlorine doses (3–6 mg/L). This translates into chemical savings, reduced waste, and lower environmental impact. Combining both steps in one reactor may also cut mixing and pumping energy compared to conventional sequential treatment.

From a regulatory standpoint, this integrated approach helps to meet stringent effluent limits for phosphorus (<0.1–0.3 mg/L), coliforms, and DBPs. Simultaneous PACl dosing reduces DBP precursors, making compliance easier [27]. In summary, the method (a) reduces capital and hydraulic complexity, (b) minimizes chemical and energy demands, and (c) simplifies operation. These features make it attractive for both new and existing plants, particularly where space is limited or high effluent quality is required. Future pilot and field studies should confirm footprint and energy savings under real flow conditions, but current results already highlight its strong potential as a compact and sustainable treatment strategy.

5. Conclusions

The integration of polyaluminum chloride (PACl) coagulation with sodium hypochlorite (NaClO) disinfection was evaluated for secondary wastewater treatment at both bench and pilot scales. The study demonstrated measurable improvements when the two processes were combined, particularly under high-mixing pilot-scale conditions. The key findings are as follows:

- The integrated approach maintained phosphorus removal (>80%) and microbial inactivation (up to 3-log total coliform reduction), while also lowering disinfection

by-product (DBP) formation compared to conventional sequential treatment. For example, haloacetic acids (HAAs) and adsorbable organic halides (AOX) were reduced by ~4–5% with PACl addition under typical operating conditions.

- Bench-scale tests confirmed that microbial inactivation was primarily driven by NaClO dose, with limited contribution from PACl. In contrast, pilot-scale experiments indicated a modest but consistent synergistic effect, where PACl addition improved coliform reduction under high-mixing conditions.
- DBP formation (THMs, HAAs, AOX, HANs, HALs, HKs) was influenced by both NaClO dose and mixing conditions. Pilot-scale operation provided more stable outcomes, with optimized mixing improving DBP control and suggesting potential for more energy-efficient operation.
- While these results highlight operational and environmental advantages of integration, the magnitude of DBP reductions was modest and the study did not directly assess DBP toxicity or long-term system reliability. Future research should address these limitations to confirm the broader health and sustainability benefits.

In summary, the integrated coagulation/disinfection approach can improve treatment performance while offering practical benefits such as reduced retention time and chemical demand. Although the observed effects are incremental rather than transformative, they support the potential of integration as a compact and resource-efficient alternative to conventional sequential treatment.

Supplementary Materials: The following supporting information can be downloaded at https://www.mdpi.com/article/10.3390/w17192867/s1, Figure S1: Soluble phosphorus removal as a function of different PACl doses; Figure S2: Normalized concentration (N/N0) of total coliform over different PACl doses.; Figure S3: Profile plots of HAL formation; Panel A: NaClO dose, Panel B: PACl dose, Panel C: contact time; Figure S4: One-factor-at-a-time effects on HK formation; Panel A: NaClO dose, Panel B: PACl dose, Panel C: contact time; Figure S5: Profile plots of THM, HAA, AOX, HAN, HAL, and HK formation; Figure S6: Actual vs. predicted values for phosphorus removal model; Figure S7: Actual vs. predicted values for fecal coliform inactivation model in batch system; Figure S8: Actual vs. predicted values for fecal coliform inactivation model in pilot system; Figure S9: Actual vs. predicted values for total coliform inactivation model in batch system; Figure S10: Actual vs. predicted values for total coliform inactivation model in pilot system; Figure S11: Actual vs. predicted values for THMs formation model in batch system; Figure S12: Actual vs. predicted values for THMs formation model in pilot system; Figure S13: Actual vs. predicted values for HAAs formation model in batch system, Figure S14: Actual vs. predicted values for HAAs formation model in pilot system; Figure S15: Actual vs. predicted values for HALs formation model in batch system; Figure S16: Actual vs. predicted values for HALs formation model in pilot system; Figure S17: Actual vs. predicted values for HKs formation model in batch system; Figure S18: Actual vs. predicted values for HKs formation model in pilot system; Table S1: Summary of the experimental design for the preliminary batch experiment; Table S2: Soluble phosphorous concentrations using various NaClO and PACl doses; Table S3: Total and fecal coliform inactivation and DBP s formation using various NaClO and PACl doses, during different mixing time over bench scale testing; Table S4: Total and fecal coliform inactivation using various NaClO and PACl doses, and various wastewater flowrate over pilot scale testing; Table S5: DBPs formation using various NaClO and PACl doses, and various wastewater flowrate over pilot scale testing; Table S6: List of monitored DBPs; Table S7: ANOVA results for phosphorus removal model; Table S8: ANOVA results for Fecal Coliform inactivation model in batch system; Table S9: ANOVA results for Fecal Coliform inactivation model in pilot system; Table S10: ANOVA results for Total Coliform inactivation model in batch system; Table S11: ANOVA results for Total Coliform inactivation model in pilot system; Table S12: ANOVA results for THMs formation model in batch system; Table S13: ANOVA results for THMs formation model in pilot system; Table S14: ANOVA results for HAAs formation model in batch system; Table S15: ANOVA

results for HAAs formation model in pilot system; Table S16: ANOVA results for HALs formation model in batch system; Table S17: ANOVA results for HALs formation model in pilot system; Table S18: ANOVA results for HKs formation model in batch system; Table S19: ANOVA results for HKs formation model in pilot system.

Author Contributions: Conceptualization, N.F., D.S. and G.M.; methodology, N.F. and D.S.; software, N.F. and D.S.; validation, N.F., D.S. and G.M.; formal analysis, N.F., D.S., R.H. and G.E.B.B.; investigation, N.F., D.S. and G.M.; resources, N.F., D.S., T.M. and G.M.; data curation, N.F., D.S. and G.M.; writing—original draft preparation, N.F.; writing—review and editing, N.F., D.S., R.H. and K.B.; visualization, N.F., D.S. and G.M.; supervision, D.S. and G.M.; project administration, N.F., D.S. and G.M.; funding acquisition, N.F., D.S. and G.M. All authors have read and agreed to the published version of the manuscript.

Funding: Programma Operativo Nazionale Ricerca e Innovazione 2014–2020: F85F20000290007, Department of Engineering for Innovation University of Salento (Fondi per la Ricerca di Base).

Data Availability Statement: The original contributions presented in this study are included in the Supplementary Material. Further inquiries can be directed to the corresponding author.

Conflicts of Interest: Author Ted Mao was employed by the company MW Technologies, Inc. and author Katherine Bell was employed by the company Hazen and Sawyer. The remaining authors declare that the research was conducted in the absence of any commercial or financial relationships that could be construed as a potential conflict of interest.

References

1. Lin, J.L.; Ika, A.R.; Tseng, C.C. Effect of In-Situ Formed Al Hydrates through Long-Term Aging on Enhanced Particle Destabilization by PACl Coagulation. *J. Environ. Sci.* **2020**, *92*, 200–210. [CrossRef]
2. Yan, M.; Wang, D.; Qu, J.; Ni, J.; Chow, C.W.K. Enhanced Coagulation for High Alkalinity and Micro-Polluted Water: The Third Way through Coagulant Optimization. *Water Res.* **2008**, *42*, 2278–2286. [CrossRef] [PubMed]
3. Ji, X.; Li, Z.; Wang, M.; Yuan, Z.; Jin, L. Response Surface Methodology Approach to Optimize Parameters for Coagulation Process Using Polyaluminum Chloride (PAC). *Water* **2024**, *16*, 1470. [CrossRef]
4. Wei, N.; Zhang, Z.; Liu, D.; Wu, Y.; Wang, J.; Wang, Q. Coagulation Behavior of Polyaluminum Chloride: Effects of pH and Coagulant Dosage. *Chin. J. Chem. Eng.* **2015**, *23*, 1041–1046. [CrossRef]
5. Liu, Z.; Wei, H.; Li, A.; Yang, H. Enhanced Coagulation of Low-Turbidity Micro-Polluted Surface Water: Properties and Optimization. *J. Environ. Manag.* **2019**, *233*, 739–747. [CrossRef]
6. Sharafi, K.; Fazlzadeh, M.; Pirsaheb, M.; Moradi, M.; Azari, A.; Sharafi, H.; Dindarloo, K.; Ghafari, H.R. NaDCC) and Sodium Hypochlorite (NaOCL): Modeling, Optimization and Comparative Analysis. *Desalination Water Treat.* **2017**, *66*, 221–228. [CrossRef]
7. Nunes, N.B.; Reis, J.O.D.; Castro, V.S.; Machado, M.A.M.; Cunha-Neto, A.D.; Figueiredo, E.E.D.S. Optimizing the Antimicrobial Activity of Sodium Hypochlorite (NaClO) over Exposure Time for the Control of *Salmonella* Spp. In Vitro. *Antibiotics* **2024**, *13*, 68. [CrossRef]
8. Zhao, H.; Hu, C.; Liu, H.; Zhao, X.; Qu, J. Role of Aluminum Speciation in the Removal of Disinfection Byproduct Precursors by a Coagulation Process. *Environ. Sci. Technol.* **2008**, *42*, 5752–5758. [CrossRef]
9. Precious Sibiya, N.; Rathilal, S.; Kweinor Tetteh, E. Coagulation Treatment of Wastewater: Kinetics and Natural Coagulant Evaluation. *Molecules* **2021**, *26*, 698. [CrossRef]
10. Smith, S.; Takács, I.; Murthy, S.; Daigger, G.T.; Szabó, A. Phosphate Complexation Model and Its Implications for Chemical Phosphorus Removal. *Water Environ. Res.* **2008**, *80*, 428–438. [CrossRef]
11. Bryndza, H.E.; Tam, W. Monomeric Metal Hydroxides, Alkoxides, and Amides of the Late Transition Metals: Synthesis, Reactions, and Thermochemistry. *Chem. Rev.* **1988**, *88*, 1163–1188. [CrossRef]
12. Plewa, M.J.; Richardson, S.D. Disinfection By-Products in Drinking Water, Recycled Water and Wastewater: Formation, Detection, Toxicity and Health Effects: Preface. *J. Environ. Sci.* **2017**, *58*, 1. [CrossRef] [PubMed]
13. Ji, Q.; Liu, H.; Hu, C.; Qu, J.; Wang, D.; Li, J. Removal of Disinfection By-Products Precursors by Polyaluminum Chloride Coagulation Coupled with Chlorination. *Sep. Purif. Technol.* **2008**, *62*, 464–469. [CrossRef]
14. Ma, M.; Liu, R.; Liu, H.; Qu, J.; Jefferson, W. Effects and Mechanisms of Pre-Chlorination on *Microcystis aeruginosa* Removal by Alum Coagulation: Significance of the Released Intracellular Organic Matter. *Sep. Purif. Technol.* **2012**, *86*, 19–25. [CrossRef]
15. Chow, C.W.K.; Van Leeuwen, J.A.; Fabris, R.; Drikas, M. Optimised Coagulation Using Aluminium Sulfate for the Removal of Dissolved Organic Carbon. *Desalination* **2009**, *245*, 120–134. [CrossRef]

16. Pramanik, B.K.; Choo, K.-H.; Pramanik, S.K.; Suja, F.; Jegatheesan, V. Comparisons between Biological Filtration and Coagulation Processes for the Removal of Dissolved Organic Nitrogen and Disinfection By-Products Precursors. *Int. Biodeterior. Biodegrad.* **2015**, *104*, 164–169. [CrossRef]
17. Shahid, A.; Khan, A.Z.; Malik, S.; Liu, C.-G.; Mehmood, M.A.; Syafiuddin, A.; Wang, N.; Zhu, H.; Boopathy, R. Advances in Green Technologies for the Removal of Effluent Organic Matter from the Urban Wastewater. *Curr. Pollut. Rep.* **2021**, *7*, 463–475. [CrossRef]
18. Zhang, F.; Wang, Y.; Chu, Y.; Gao, B.; Yue, Q.; Yang, Z.; Li, Q. Reduction of Organic Matter and Trihalomethane Formation Potential in Reclaimed Water from Treated Municipal Wastewater by Coagulation and Adsorption. *Chem. Eng. J.* **2013**, *223*, 696–703. [CrossRef]
19. Ding, S.; Chu, W.; Bond, T.; Cao, Z.; Xu, B.; Gao, N. Contribution of Amide-Based Coagulant Polyacrylamide as Precursors of Haloacetamides and Other Disinfection by-Products. *Chem. Eng. J.* **2018**, *350*, 356–363. [CrossRef]
20. Fallah, N.; Bell, K.; Mao, T.; Hofmann, R.; Bossoni, G.E.B.; Santoro, D.; Mele, G. Chemical Disinfection of Secondary Municipal Wastewater Effluents: Optimizing CT Dose and Tailing Effects through High-intensity Mixing. *Water Environ. Res.* **2025**, *97*, e70066. [CrossRef]
21. Ghernaout, D. Enhanced Coagulation: Promising Findings and Challenges. *OALib* **2020**, *7*, 1–19. [CrossRef]
22. Hahn, H.; Hoffman, E.; Odegaard, H. Chemical Water and Wastewater Treatment VIII. *Water Intell. Online* **2015**, *4*, 9781780402840. [CrossRef]
23. Wang, H.; Yu, L.-Q.; Chen, S.-N.; Liu, M.; Fan, N.-S.; Huang, B.-C.; Jin, R.-C. Coagulation Enhanced High-Rate Contact-Stabilization Process for Pretreatment of Municipal Wastewater: Simultaneous Organic Capture and Phosphorus Removal. *Sep. Purif. Technol.* **2022**, *298*, 121669. [CrossRef]
24. Zhang, Y.; Li, M.; Zhang, G.; Liu, W.; Xu, J.; Tian, Y.; Wang, Y.; Xie, X.; Peng, Z.; Li, A.; et al. Efficient Treatment of the Starch Wastewater by Enhanced Flocculation–Coagulation of Environmentally Benign Materials. *Sep. Purif. Technol.* **2023**, *307*, 122788. [CrossRef]
25. Hu, C.; Liu, H.; Qu, J.; Wang, Y. Coagulation and Disinfection Efficiency of an Electrochemically Prepared Dual-Function Reagent in Municipal Wastewater. *J. Environ. Sci. Health Part A* **2006**, *41*, 2387–2398. [CrossRef]
26. Song, J.; Wang, J.; Wang, D. Changes in the Structural Characteristics of EfOM during Coagulation by Aluminum Chloride and the Effect on the Formation of Disinfection Byproducts. *J. Environ. Manag.* **2023**, *326*, 116850. [CrossRef]
27. Golfinopoulos, S.K.; Nikolaou, A.D.; Alexakis, D.E. Innovative Approaches for Minimizing Disinfection Byproducts (DBPs) in Water Treatment: Challenges and Trends. *Appl. Sci.* **2024**, *14*, 8153. [CrossRef]
28. Wang, J.; Yue, W.; Wang, Z.; Bai, Y.; Song, J. Removal Effect of Trihalomethanes (THMs) and Halogenated Acetic Acids (HAAs) Precursors in Reclaimed Water by Polyaluminum Chloride (PACl) Coagulation. *Water Sci. Technol.* **2023**, *87*, 672–684. [CrossRef]
29. Wang, P.; Ding, S.; Xiao, R.; An, G.; Fang, C.; Chu, W. Enhanced Coagulation for Mitigation of Disinfection By-Product Precursors: A Review. *Adv. Colloid Interface Sci.* **2021**, *296*, 102518. [CrossRef]
30. Krasner, S.W.; Westerhoff, P.; Chen, B.; Rittmann, B.E.; Nam, S.-N.; Amy, G. Impact of Wastewater Treatment Processes on Organic Carbon, Organic Nitrogen, and DBP Precursors in Effluent Organic Matter. *Environ. Sci. Technol.* **2009**, *43*, 2911–2918. [CrossRef]
31. Lin, J.-L.; Ika, A.R. Minimization of Halogenated DBP Precursors by Enhanced PACl Coagulation: The Impact of Organic Molecule Fraction Changes on DBP Precursors Destabilization with Al Hydrates. *Sci. Total Environ.* **2020**, *703*, 134936. [CrossRef]
32. Kalita, I.; Kamilaris, A.; Havinga, P.; Reva, I. Assessing the Health Impact of Disinfection Byproducts in Drinking Water. *ACS EST Water* **2024**, *4*, 1564–1578. [CrossRef]
33. Luan, X.; Liu, X.; Fang, C.; Chu, W.; Xu, Z. Ecotoxicological Effects of Disinfected Wastewater Effluents: A Short Review of in Vivo Toxicity Bioassays on Aquatic Organisms. *Environ. Sci. Water Res. Technol.* **2020**, *6*, 2275–2286. [CrossRef]
34. Sun, G.; Li, Y. Exposure to DBP Induces the Toxicity in Early Development and Adverse Effects on Cardiac Development in Zebrafish (*Danio rerio*). *Chemosphere* **2019**, *218*, 76–82. [CrossRef]
35. Wang, G.; Wang, J.; Zhu, L.; Wang, J.; Li, H.; Zhang, Y.; Liu, W.; Gao, J. Oxidative Damage and Genetic Toxicity Induced by DBP in Earthworms (*Eisenia fetida*). *Arch. Environ. Contam. Toxicol.* **2018**, *74*, 527–538. [CrossRef]
36. Yuan, L.; Liu, J.; Huang, Y.; Shen, G.; Pang, S.; Wang, C.; Li, Y.; Mu, X. Integrated Toxicity Assessment of DEHP and DBP toward Aquatic Ecosystem Based on Multiple Trophic Model Assays. *Environ. Sci. Pollut. Res.* **2022**, *29*, 87402–87412. [CrossRef]